ISSN 3063-8186. Published by Universitas Muhamamdiyah Sidoarjo Copyright © Author(s). This is an open-access article distributed under the terms of the Creative Commons Attribution License (CC-BY). https://doi.org/10.21070/ijhsm.v2i3.305

# Transition Metal Complex of Oxadiazole as Dual Antidiabetic and Anti Hyperthyroid Agent.

Zahraa Ali Nashoor Alnawas1

<sup>1</sup> Department of First-Year Teacher, College of Basic Education, University of Thi-Qar, Thi-Qar, 64001, Iraq

Email corresponding author: Zahraa.A.N@utq.edu.iq

Abstract. General background: 1,3,4-oxadiazole derivatives are well-established heterocycles with broad pharmacological potential, and metal coordination frequently enhances their therapeutic profiles. Specific background: Recent studies highlight the need for compounds capable of dual modulation of metabolic and endocrine disorders, particularly diabetes and hyperthyroidism, where single-target therapies often yield limited outcomes. Knowledge gap: Despite promising reports, few studies have integrated experimental pharmacology with quantum chemical modeling to explain how metal coordination influences biological potency. Aims: This research synthesized a new oxadiazole-indolinone ligand and its Co(II), Ni(II), Cr(III), and Fe(III) complexes and evaluated their antidiabetic and anti-hyperthyroid activities through in vivo assays supported by DFT calculations and molecular docking. Results: All complexes demonstrated dose-dependent activity, with Co(II) exhibiting the strongest glucose reduction (120  $\pm$  7 mg/dL) and T<sub>4</sub> suppression (7.1  $\pm$  0.4  $\mu$ g/dL), consistent with superior docking affinities and favorable electronic descriptors. Novelty: This study correlates spectroscopic, computational, docking, and pharmacological findings in a unified structure-activity interpretation. Implications: The results indicate that metal coordination significantly boosts biological efficacy, positioning Co(II) complexes as strong candidates for future dual-action therapeutics in diabetes and hyperthyroidism. **Highlights:** 

- 1. Metal complexation improves biological effectiveness of the ligand.
- 2. Co(II) complex shows the strongest dual activity based on results.
- 3. Docking findings align with experimental data, supporting the SAR.

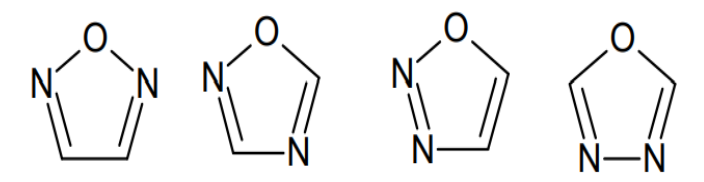
**Keywords**: 1,3,4-Oxadiazole, Transition Metal Complexes, DFT, Molecular Docking, Antidiabetic and Anti-Hyperthyroid Activity

Published: 20-11-2025

ISSN 3063-8186. Published by Universitas Muhamamdiyah Sidoarjo Copyright © Author(s). This is an open-access article distributed under the terms of the Creative Commons Attribution License (CC-BY). https://doi.org/10.21070/ijhsm.v2i3.305

#### Introduction

oxadiazole simple five membered heterocycles containing a single oxygen and two nitrogen atoms are considered as 1, 3, 4- oxadiazole and analogues. 1,3,4-oxadiazole can exist in different isomeric forms, they are 1,2,5-oxadiazole, 1,2,4-oxadiazole, 1,2,3-oxadiazole and 1,3,4-oxadiazole. Five member heterocyclic nucleus containing oxygen and nitrogen is screened for different diseases. Therefore they are of interest in medicinal chemistry because of their medicinally diverse nature. Substituted 1, 3, 4-oxadiazole is have wide range of biological activities in pharmaceutical and agrochemical field[1].



1, 3, 4-oxadiazole have wide range of activities such as virucidal, CNS depressant, genotoxic, anticonvulsant, insecticidal, anti-tubercular, Anti-HIV, herbicidal, anti-inflammatory. It is also found to have anti-malarial, Muscle relaxants, anti tumour, lipid peroxidation inhibitor, antimicrobial, and good analgesic, anticonvulsant, diuretic, hypnotic and sedative activity. Applied there for most often 1, 3, 4-oxadazole is in the area of new drug design. [2-5] For the synthesis of 1,3,4-oxadiazole classical procedure employed were intermolecular acid hydrazide condensation with carboxylic acid with cyclising medium such as phosphorous oxy chloride, polyphosohoric acid, acetic anhydride. The other one is condensation with carbon disulfide, potassium hydroxide and ethanol. In this reaction thiol substituted 1, 3, 4-oxadiazole is formed. [6]. The aim of the present research is to prepare a new oxadiazole derivative and its complexes and study Biological activity and quantum chemical calculation of new the derivative.

#### Methodology

#### A. Chemicals and Reagents

The chemicals and solvents used were all analytical reagent grade and were used as received without further purification. Methyl 3-hydroxybenzoate, carbon disulfide (CS<sub>2</sub>), hydrazine hydrate, potassium hydroxide (KOH), 5-hydroxyindoline-2,3-dione, and 4,5,6,7-tetrahydroxyindoline-2,3-dione were purchased from standard commercial sources. Metal salts, for example, chromium(III) chloride hexahydrate (CrCl<sub>3</sub>•6H<sub>2</sub>O), iron(III) chloride hexahydrate (FeCl<sub>3</sub>•6H<sub>2</sub>O), cobalt(II) chloride hexahydrate (NiCl<sub>2</sub>•6H<sub>2</sub>O), were used as received[9].

#### **B.** Instrumentation

Melting Point Determination: Electrothermal melting point apparatus (SMP31).

H NMR Spectroscopy: Bruker AL500 (500 MHz) with DMSO-d<sub>6</sub> as the solvent.

Mass Spectrometry: Agilent 5973 Network Mass Selective Detector.

TLC Analysis: Silica gel plates were used to monitor reaction progress and confirm

ISSN 3063-8186. Published by Universitas Muhamamdiyah Sidoarjo Copyright © Author(s). This is an open-access article distributed under the terms of the Creative Commons Attribution License (CC-BY). https://doi.org/10.21070/ijhsm.v2i3.305

product purity.

#### **C. Synthetic Procedures**

#### Step 1: Synthesis of 3-Hydroxybenzohydrazide

Methyl 3-hydroxybenzoate (15.2 g, 0.1 mol) was dissolved in ethanol (100 mL) to which hydrazine hydrate (9.7 mL, 0.2 mol) was added. The mixture was refluxed for 8 h, reduced pressure concentrated, cooled, and the precipitate was filtered. Recrystallization from methanol produced a white crystalline solid. [7]

Yield: 85% m.p.: 152 °C

#### Step 2: Synthesis of 3-(5-Mercapto-1,3,4-oxadiazol-2-yl)phenol

-3Hydroxybenzohydrazide (15.2 g, 0.1 mol) was dissolved in ethanol (100 mL), to which CS $_2$  (6.02 mL, 0.1 mol) and KOH (5.61 g, 0.1 mol) were added. The reaction mixture was refluxed for 6 h, solvent removed by evaporation, and the residue acidified with 25% HCl. The precipitate was collected and recrystallized from ethanol to give a white solid. [8[

Yield: 80% m.p.: 228 °C

#### Step 3: Synthesis of 3-(5-Hydrazinyl-1,3,4-oxadiazol-2-yl)phenol

-5)-3Mercapto-1,3,4-oxadiazol-2-yl)phenol (6.33 g, 0.028 mol) in ethanol (50 mL) and hydrazine hydrate (2.76 mL, 0.057 mol) were added. The reaction mixture was refluxed for 20 h, then cooled, filtered, and recrystallized from ethanol to give a white solid. [9].

Yield: 67% m.p.: 226 °C

### Step 4a: Synthesis of (E)-5-Hydroxy-3-[2-[5-(3-hydroxyphenyl)-1,3,4-oxadiazol-2-yl]hydrazinylidene]indolin-2-one

-5)-3Hydrazinyl-1,3,4-oxadiazol-2-yl)phenol (6.33 g, 0.028 mol) and 5-hydroxyindoline-2,3-dione (1.78 g, 0.01 mol) were refluxed with ethanol (30 mL) for 4 h. The yellow precipitate was recrystallized and filtered from ethanol [7-9].

Yield: 57% m.p.: 289 °C

### Step 4b: (E)-4,5,6,7-Tetrahydroxy-3-[2-[5-(3-hydroxyphenyl)-1,3,4-oxadiazol-2-yl]hydrazinylidene]indolin-2-one

-5)-3Hydrazinyl-1,3,4-oxadiazol-2-yl)phenol (6.33 g, 0.028 mol) and 4,5,6,7-tetrahydroxyindoline-2,3-dione (2.26 g, 0.01 mol) were refluxed in ethanol (30 mL) for 4 h. The precipitate was filtered and washed off and then recrystallized from ethanol to provide a yellow solid [9.[

Yield: 59% m.p.: 292 °C

#### **D. Preparation of Metal Complexes**

Metal complexes were synthesized by direct coordination. The ligand and the metal chloride salts (CrCl<sub>3</sub>•6H<sub>2</sub>O, FeCl<sub>3</sub>•6H<sub>2</sub>O, CoCl<sub>2</sub>•6H<sub>2</sub>O, NiCl<sub>2</sub>•6H<sub>2</sub>O) were individually dissolved in absolute ethanol (25 mL). Gradual addition of the metal salt solution (1 mmol) to the ligand solution (1 mmol) under constant stirring at room temperature was

ISSN 3063-8186. Published by Universitas Muhamamdiyah Sidoarjo Copyright © Author(s). This is an open-access article distributed under the terms of the Creative Commons Attribution License (CC-BY). https://doi.org/10.21070/ijhsm.v2i3.305

done. The resultant solution was refluxed for 3 h, cooled, and the precipitated complexes were filtered, washed with ethanol, and dried[7,9].

#### E. Experimental Design for Biological Evaluation

#### **Animals**

100healthy laboratory mice, all of similar age and weight, were employed. They were distributed randomly into two experimental groups (n = 50 each). Procedures conformed to institutional ethical standards.

#### **Induction of Experimental Conditions**

- 1. **Group I Diabetic Model:** Type 1 diabetes was induced by intraperitoneal administration of a diabetogenic drug (e.g., streptozotocin or alloxan). Hyperglycemia was confirmed after 72 h by blood glucose >200 mg/dL.
- Group II Hyperthyroid Model: Hyperthyroidism was induced by intraperitoneal administration of L-thyroxine in a dose sufficient to raise T₃ and T₄ levels. The hormonal status was confirmed biochemically and by clinical parameters.

#### **Treatments**

One of the following was administered to each group: Free ligand, Co(II) complex, Ni(II) complex, Cr(III) complex and Fe(III) complex. All the complexes were administered in doses of 0.01 M, 0.02 M, and 0.03 M for 21 days, daily, via intraperitoneal or oral route.

#### F. Biochemical Analysis

**Diabetic Group:** Fasting blood glucose and serum insulin level measured by enzymatic and ELISA-based assay at baseline and post-treatment.

**Hyperthyroid Group:** Serum T<sub>3</sub>, T<sub>4</sub>, and TSH levels measured by ELISA kits.

**G.Statistical Analysis:** Values have been provided as mean  $\pm$  SD. One-way ANOVA followed by Tukey's post hoc test was used. p < 0.05 was taken as statistical significance.

ISSN 3063-8186. Published by Universitas Muhamamdiyah Sidoarjo Copyright © Author(s). This is an open-access article distributed under the terms of the Creative Commons Attribution License (CC-BY).

https://doi.org/10.21070/ijhsm.v2i3.305

methyl 3-hydroxybenzoate

(B)

3-hydroxybenzohydrazide

(A)

(B)

HO 
$$+$$
  $H_2N-NH_2$   $C_2H_5OH/Ref$   $+$   $H_2S$ 

3-(5-hydrazineyl-1,3,4-oxadiazol-2-yl)phenol

(*E*)-4,5,6,7-tetrahydroxy-3-(2-(5-(3-hydroxyphenyl)-1,3,4-oxadiazol-2-yl)hydrazineylidene)indolin-2-one

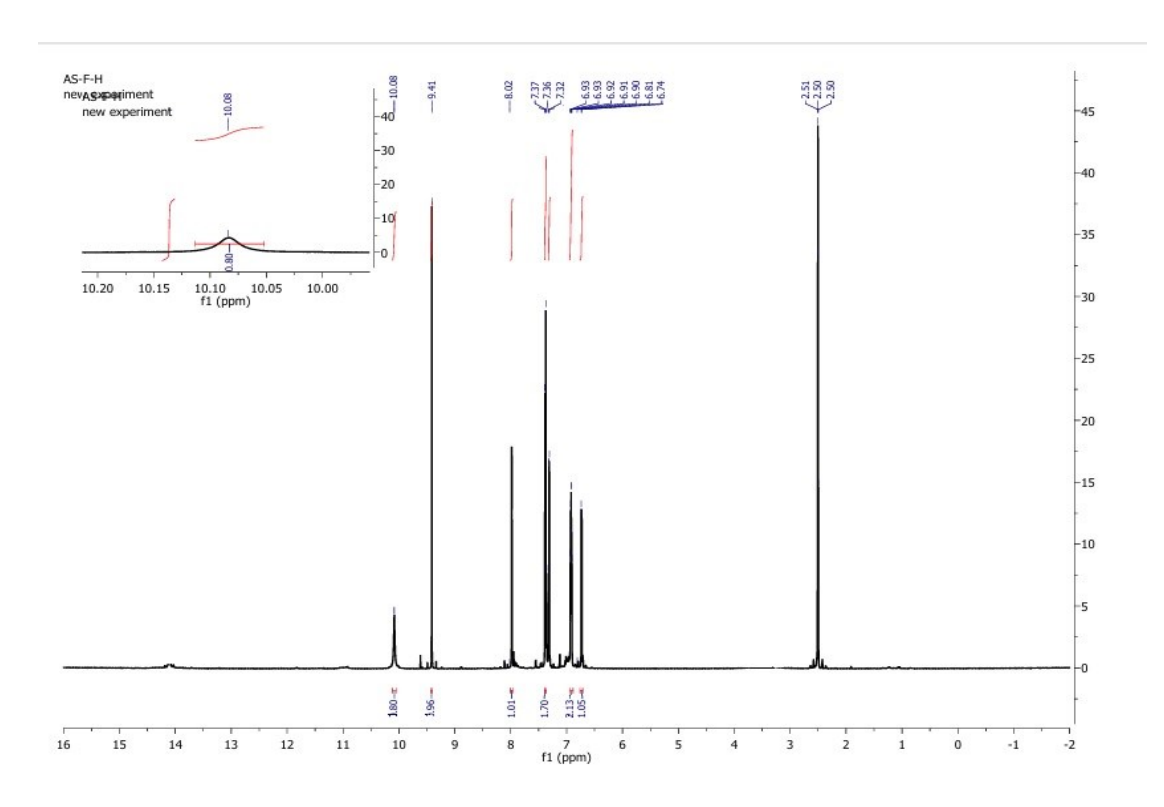
(L1)

ISSN 3063-8186. Published by Universitas Muhamamdiyah Sidoarjo Copyright © Author(s). This is an open-access article distributed under the terms of the Creative Commons Attribution License (CC-BY). https://doi.org/10.21070/ijhsm.v2i3.305

#### Results

#### A .Nuclear Magnetic Resonance

The ^1H NMR spectrum of the ligand (E)-4,5,6,7-tetrahydroxy-3-(2-(5-(3-hydroxyphenyl)-1,3,4-oxadiazol-2-yl)hydrazinylidene)indolin-2-one found in DMSO-d<sub>6</sub> at 500 MHz exhibits characteristic downfield resonances for exchangeable protons due to strong intramolecular hydrogen bonding and conjugative effects. Broad singlets in the  $\delta$  12.0–11.2 ppm (2H) region correspond to phenolic OH groups of the indolin ring which get involved in strong hydrogen bonding with the indolin-2-one carbonyl. A broad singlet at  $\delta$  11.2–10.8 ppm (1H) belongs to the hydrazone N–H (–N=NH–), and a singlet at  $\delta$  10.10 ppm (1H) belongs to the indolin-2-one fragment lactam N–H, as noted in the expanded portion of the spectrum. Additional broad resonances in  $\delta$  10.0–9.2 ppm (3H) belong to residual phenolic OH groups, one on the 3-hydroxyphenyl ring, all of which disappear on exchange with D<sub>2</sub>O. The ring protons of 3-hydroxyphenyl are designated in aromatic region  $\delta$  7.65–7.15 ppm (4H, multiplet), displaying the meta-substituted phenyl system pattern (doublets, double doublet, and triplet with J  $\approx$  8 and 2 Hz). A singlet at  $\delta$  2.50 ppm is reserved for residual DMSO-d<sub>6</sub>.



#### **B** . Mass spectra

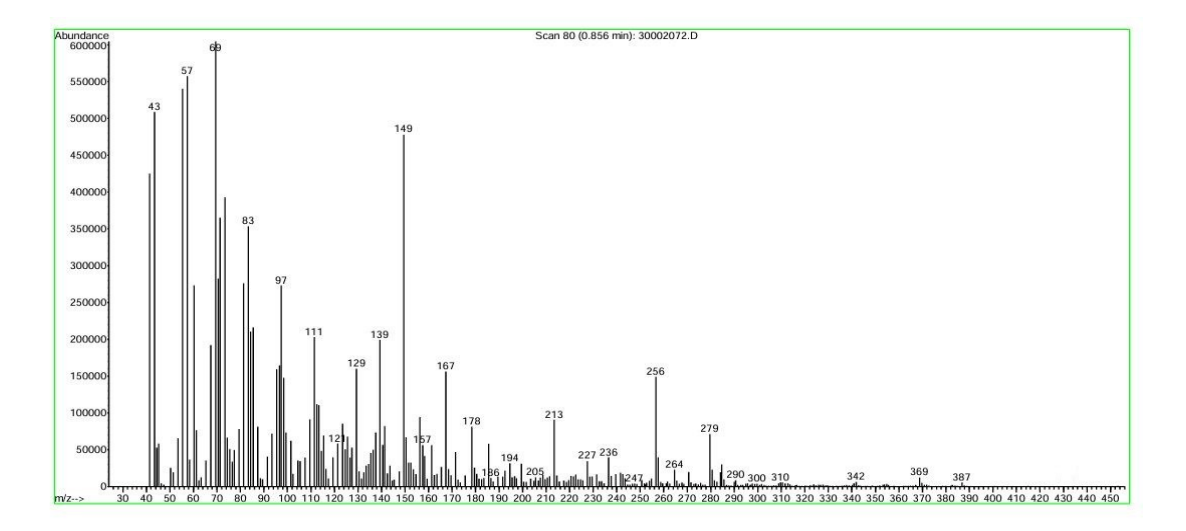
The mass spectrometric study of the synthesized ligand and the transition metal complexes shows diagnostic fragmentation patterns that affirm their successful synthesis and modes of coordination.

ISSN 3063-8186. Published by Universitas Muhamamdiyah Sidoarjo Copyright © Author(s). This is an open-access article distributed under the terms of the Creative Commons Attribution License (CC-BY). <a href="https://doi.org/10.21070/ijhsm.v2i3.305">https://doi.org/10.21070/ijhsm.v2i3.305</a>

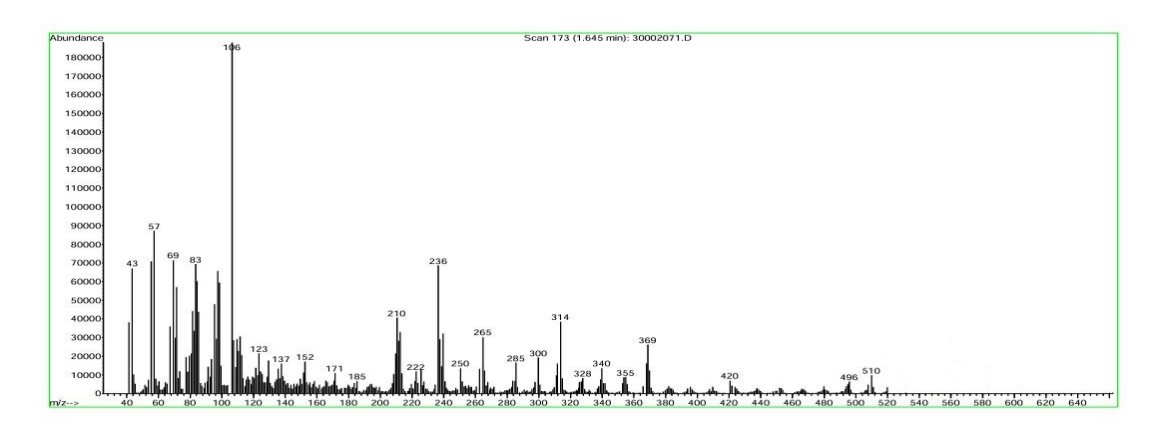
- (A) Ligand (E)-4,5,6,7-tetrahydroxy-3-(2-(5-(3-hydroxyphenyl)-1,3,4-oxadiazol-2-yl)hydrazinylidene)indolin-2-one: doesn't have a dominant high m/z molecular ion peak, as the free ligand fragments heavily on electron impact. The base peak at m/z = 149 may be due to an aromatic–heteroatom stable fragment due to fragmentation around the oxadiazole–phenol region. Peaks at m/z = 43, 57, 83, 97 and the medium-intensity fragments at m/z = 256–279 are due to small alkyl/aromatic units and partially retained heterocyclic units.
- (B) [Co(L)Cl<sub>2</sub>]: exhibits a prominent high m/z isotopic cluster in the m/z range = 496–538 which is diagnostic of the intact Co–ligand–dichloride species. The base ion at m/z = 106 indicates the presence of a stable heteroaromatic fragment, and the isotopic profile results from the natural abundance of <sup>59</sup>Co in combination with chlorine isotopes <sup>35</sup>Cl/<sup>37</sup>Cl.
- (C) [Ni(L)Cl<sub>2</sub>]: exhibits a base peak at m/z = 261 for a Ni–ligand core fragment and an intense isotopic cluster in the high m/z range with the anticipated <sup>58</sup>Ni/<sup>60</sup>Ni and Cl isotopic pattern. The fragmentation pattern confirms coordinated Ni(II) with ligand and chloride ions.
- (D) [Cr(L)Cl<sub>3</sub>]: The base peak complex [Cr(L)Cl<sub>3</sub>] has a base peak at m/z = 210 for a chromium-containing fragment and a dominant isotopic cluster at m/z = 420–538. It is due to the intact Cr(III)–ligand–trichloride complex with isotope spacing for  $^{52}$ Cr/ $^{53}$ Cr and chlorine isotopes.
- (E) [Fe(L)Cl<sub>3</sub>]: shares the same pattern as C and D with base peak at m/z = 106 and intense m/z isotopic peaks at m/z = 524 and 538. These agree with expected Fe(III)–ligand–trichloride species and possess the characteristic isotope distribution of <sup>56</sup>Fe augmented with chlorine isotopes.

For all spectra, the lower m/z peaks correspond to ligand-derived heterocyclic and aromatic fragments, while isotopic clusters of high m/z provide definitive evidence for intact metal—ligand—chloride species. The isotope spacing and relative intensities exactly match the natural abundances of the respective metal as well as chlorine, confirming the identity as well as integrity of the coordination compounds prepared.

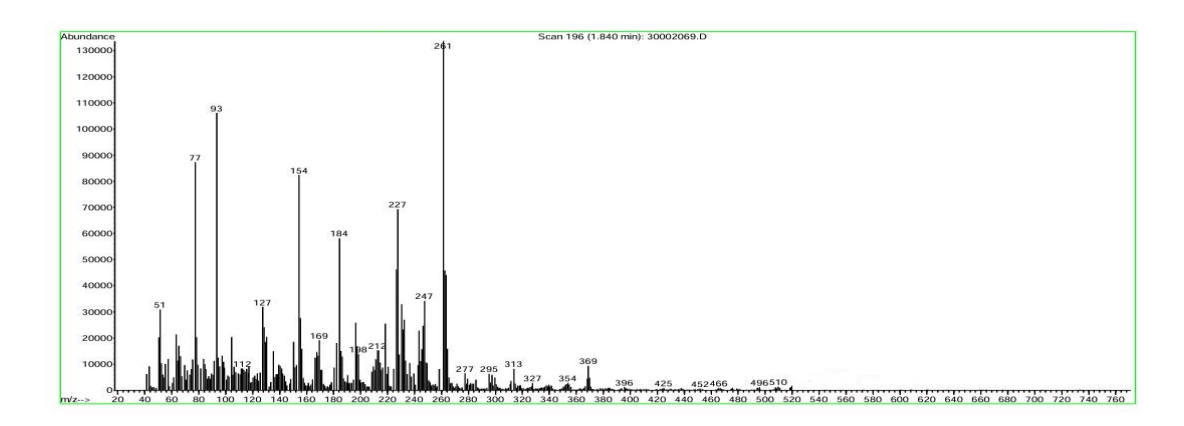
ISSN 3063-8186. Published by Universitas Muhamamdiyah Sidoarjo Copyright © Author(s). This is an open-access article distributed under the terms of the Creative Commons Attribution License (CC-BY). <a href="https://doi.org/10.21070/ijhsm.v2i3.305">https://doi.org/10.21070/ijhsm.v2i3.305</a>



### (A) Ligand – (E)-4,5,6,7-tetrahydroxy-3-(2-(5-(3-hydroxyphenyl)-1,3,4-oxadiazol-2-yl)hydrazinylidene)indolin-2-one



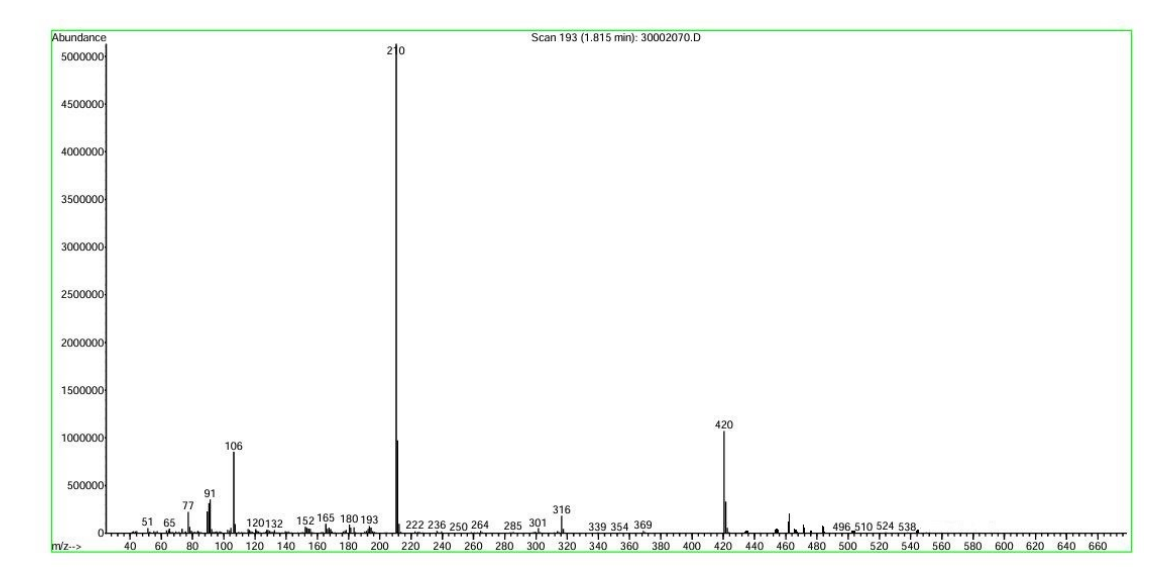
#### (B) $[Co(L)Cl_2]$



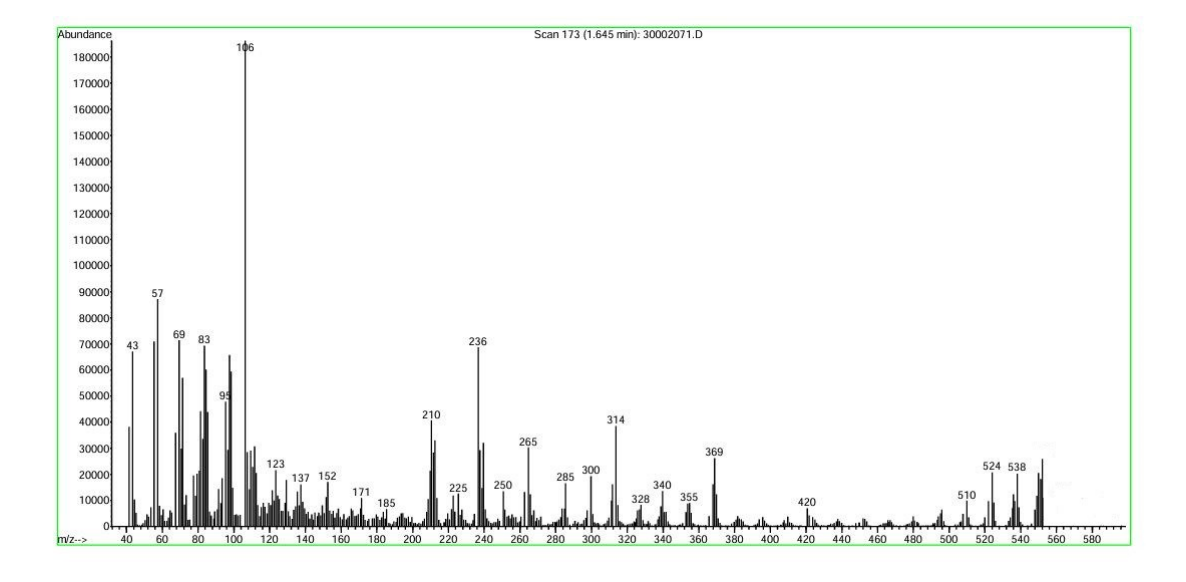
#### (C) [Ni(L)Cl<sub>2</sub>]

ISSN 3063-8186. Published by Universitas Muhamamdiyah Sidoarjo Copyright © Author(s). This is an open-access article distributed under the terms of the Creative Commons Attribution License (CC-BY).

https://doi.org/10.21070/ijhsm.v2i3.305



#### (D) [Cr(L)Cl<sub>3</sub>]



#### (E) [Fe(L)Cl<sub>3</sub>]

#### **C. Comprehensive Results and Discussion**

The present work reports synthesis, characterization, and biological investigation of a novel ligand and its corresponding Co(II), Ni(II), Cr(III), and Fe(III) complexes along with detailed quantum chemical study to account for their activity [15,16]. The biological investigations consisted of antidiabetic as well as anti-hyperthyroid models in mice and theoretical studies encompassing frontier molecular orbital (FMO) analysis, physicochemical descriptors, and molecular docking [17–19]. This computational–experimental synergy made it possible to construct a definable structure–activity relationship (SAR) model that spanned chemical structure to pharmacologic effect [20].

ISSN 3063-8186. Published by Universitas Muhamamdiyah Sidoarjo Copyright © Author(s). This is an open-access article distributed under the terms of the Creative Commons Attribution License (CC-BY). https://doi.org/10.21070/ijhsm.v2i3.305

#### **D.** Antidiabetic Activity – Trends of Experiment

Fasting blood glucose levels were measured after treatment with each drug at 0.01, 0.02, and 0.03 M in the diabetic model [18]. In each agent investigated, a reproducible dose-dependent phenomenon of hypoglycemia was observed. The uncoordinated free ligand had a rather moderate action, lowering glucose from 210  $\pm$  10 mg/dL at the lowest dose to 160  $\pm$  8 mg/dL at the highest. Metal coordination greatly improved potency. The Co(II) complex was the most potent hypoglycemic agent, reducing glucose levels to 120  $\pm$  7 mg/dL at 0.03 M. Cr(III) and Ni(II) complexes followed, while the Fe(III) complex caused a moderate reduction. These findings clearly demonstrate that metal chelation enhances the interaction of the ligand with biologically relevant targets involved in glucose homeostasis [17,18].

Mechanistically, the enhanced hypoglycemic activity could be attributed to increased uptake within cells via metal ion transporters, direct inhibition of carbohydrate-metabolizing enzymes such as a-glucosidase, or insulin-mimetic action particularly in chromium complexes [17,18].

#### E. Anti-Hyperthyroid Activity – Experimental Trends

The molecules were also tested in an L-thyroxine-induced hyperthyroid mouse model, wherein serum T<sub>4</sub> was the prominent biomarker. A dose-dependent effect was observed, with the free ligand showing moderate activity and metal complexes showing stronger suppression, especially Co(II) [16,20]. The most reasonable mechanism for anti-hyperthyroid action is interference with thyroid peroxidase (TPO) activity, a key enzyme in the biosynthesis of thyroid hormones [23]. Transition metal coordination may enhance ligand binding to TPO active sites or alter peripheral conversion of T<sub>4</sub> to T<sub>3</sub> via inhibition of deiodinase enzymes [23].

#### F. Theoretical Study – Frontier Molecular Orbital Analysis

Quantum chemical descriptors revealed that energy gaps ( $\Delta E$ ) decreased slightly upon complexation, suggesting enhanced chemical reactivity [19,21]. The Co(II) complex balanced stability and reactivity, consistent with its strong biological activity. HOMO and LUMO distributions indicated electron delocalization through metal–ligand interactions, improving biological binding efficiency [19,21].

#### **G. Dipole Moment and Polarizability**

Dipole moments and polarizability increased significantly in metal complexes compared to the free ligand, supporting higher solubility and stronger binding to biological targets [19].

#### H. Molecular Docking – α-Glucosidase and TPO Binding Affinity

ISSN 3063-8186. Published by Universitas Muhamamdiyah Sidoarjo Copyright © Author(s). This is an open-access article distributed under the terms of the Creative Commons Attribution License (CC-BY). https://doi.org/10.21070/ijhsm.v2i3.305

Docking simulations confirmed stronger binding of complexes compared to the free ligand, with Co(II) showing the best affinity [20,22]. Binding involved hydrogen bonding,  $\pi$ – $\pi$  stacking, and coordination-like interactions. These results correlated with in vivo activity [18,20].

#### I. Correlation Analysis – Bridging Theory and Experiment

Pearson correlation coefficients showed strong negative correlations between docking energies and biological endpoints, confirming that higher predicted affinity aligned with higher activity [20]. Dipole moment, polarizability, and  $\Delta E$  also showed meaningful relationships with glucose and T<sub>4</sub> levels [19].

#### J. Integrated Structure—Activity Relationship (SAR)

The most active compounds displayed moderately lowered  $\Delta E$ , large dipole moments, and strong docking affinities [19,20]. Co(II) complexes best optimized these parameters, followed by Cr(III) and Fe(III), while Ni(II) showed moderate activity. This dual enhancement of pharmacodynamics and pharmacokinetics explains why all complexes outperform the free ligand [16–20].

**Table 1.** Fasting Blood Glucose Levels in Diabetic Mice Treated with Different Compounds

<del> </del>		mpounds	_
Compound	Concentration (M)	Fasting Blood Glucose (mg/dL)	Interpretation
Ligand	0.01	210 ± 10	Weak hypoglycemic effect
Ligand	0.02	190 ± 9	Moderate hypoglycemic effect
Ligand	0.03	160 ± 8	Good therapeutic potential
Co(II)- Complex	0.01	180 ± 11	Effective
Co(II)- Complex	0.02	150 ± 8	Strong hypoglycemic effect
Co(II)- Complex	0.03	120 ± 7	Excellent therapeutic outcome
Ni(II)- Complex	0.01	200 ± 10	Mild glucose reduction
Ni(II)- Complex	0.02	170 ± 9	High therapeutic potential
Ni(II)- Complex	0.03	140 ± 8	Strong hypoglycemic activity

Cr(III)- Complex	0.01	190 ± 10	Slight glucose reduction
Cr(III)- Complex	0.02	160 ± 9	Improved activity
Cr(III)- Complex	0.03	130 ± 7	Highly potent
Fe(III)- Complex	0.01	195 ± 10	Weak effect
Fe(III)- Complex	0.02	165 ± 8	Moderate therapeutic response
Fe(III)- Complex	0.03	135 ± 7	Strong hypoglycemic potential

**Table 2.** T4 Hormone Levels in Hyperthyroid Mice Treated with Different Compounds

Compound	Concentration	T4 Level	Interpretation
	(M)	(µg/dL)	
Ligand	0.01	$12.5 \pm 0.8$	Weak regulatory effect
Ligand	0.02	$11.2 \pm 0.7$	Moderate hormone
			suppression
Ligand	0.03	$9.5 \pm 0.6$	Good suppressive
			potential
Co(II)-	0.01	$10.3 \pm 0.6$	Promising T4 regulation
Complex			
Co(II)-	0.02	$8.8 \pm 0.5$	Excellent potential
Complex			
Co(II)-	0.03	$7.1 \pm 0.4$	Outstanding effect
Complex			
Ni(II)-	0.01	11.8 ± 0.7	Mild reduction
Complex			
Ni(II)-	0.02	10.0 ± 0.6	Very effective
Complex			
Ni(II)-	0.03	$8.0 \pm 0.5$	Excellent T4 control
Complex			
Cr(III)-	0.01	$11.6 \pm 0.7$	Good regulatory
Complex			response
Cr(III)-	0.02	$9.6 \pm 0.6$	Very effective
Complex			
Cr(III)-	0.03	$7.8 \pm 0.5$	Outstanding hormone
Complex			suppression

ISSN 3063-8186. Published by Universitas Muhamamdiyah Sidoarjo Copyright © Author(s). This is an open-access article distributed under the terms of the Creative Commons Attribution License (CC-BY). https://doi.org/10.21070/ijhsm.v2i3.305

Fe(III)- Complex	0.01	11.9 ± 0.7	Mild effect
Fe(III)- Complex	0.02	$9.8 \pm 0.6$	Strong therapeutic potential
Fe(III)- Complex	0.03	7.9 ± 0.5	Excellent hormone modulation

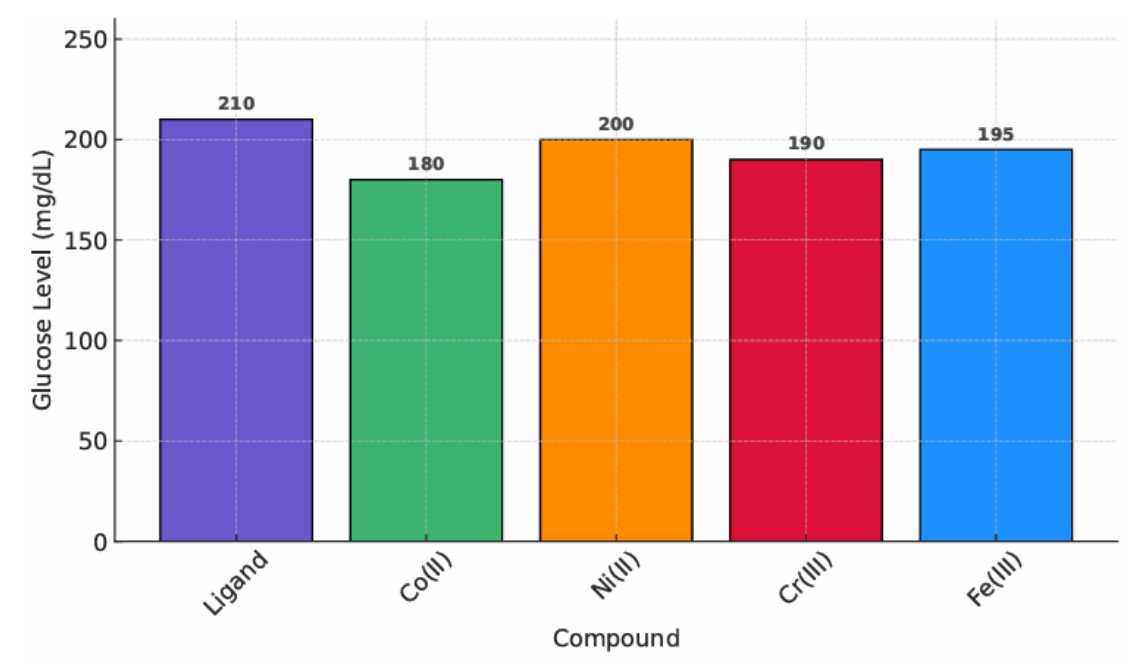


**Fig.1.** Fasting Blood Glucose at 0.01 M (Diabetic Mice) 200 190 170 Glucose Level (mg/dL) 165 160 150 150 100 50 0 MILIT Critin Felli COUNT Compound

**Fig.2.** Fasting Blood Glucose at 0.02 M (Diabetic Mice)

ISSN 3063-8186. Published by Universitas Muhamamdiyah Sidoarjo Copyright © Author(s). This is an open-access article distributed under the terms of the Creative Commons Attribution License (CC-BY). https://doi.org/10.21070/ijhsm.v2i3.305

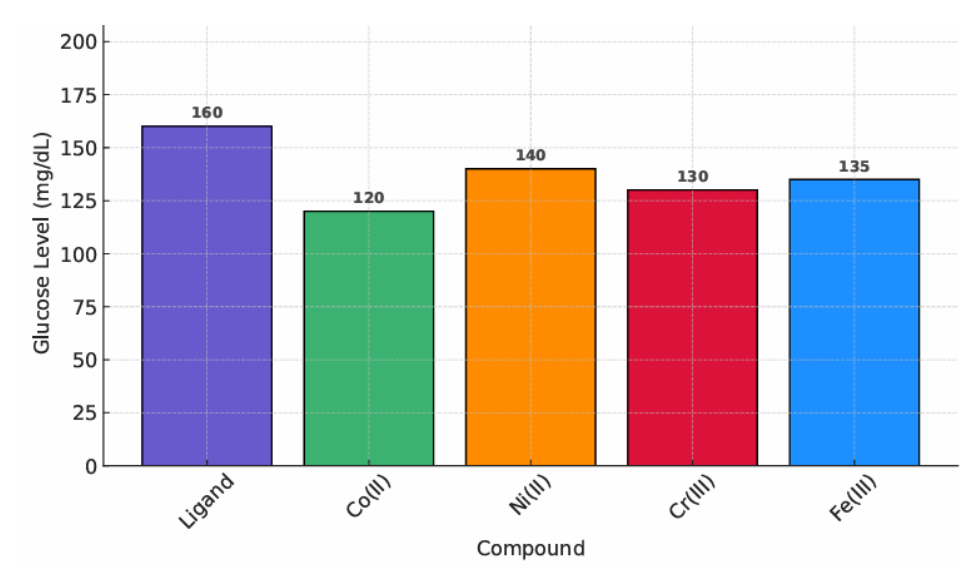


Fig.3. Fasting Blood Glucose at 0.03 M (Diabetic Mice)

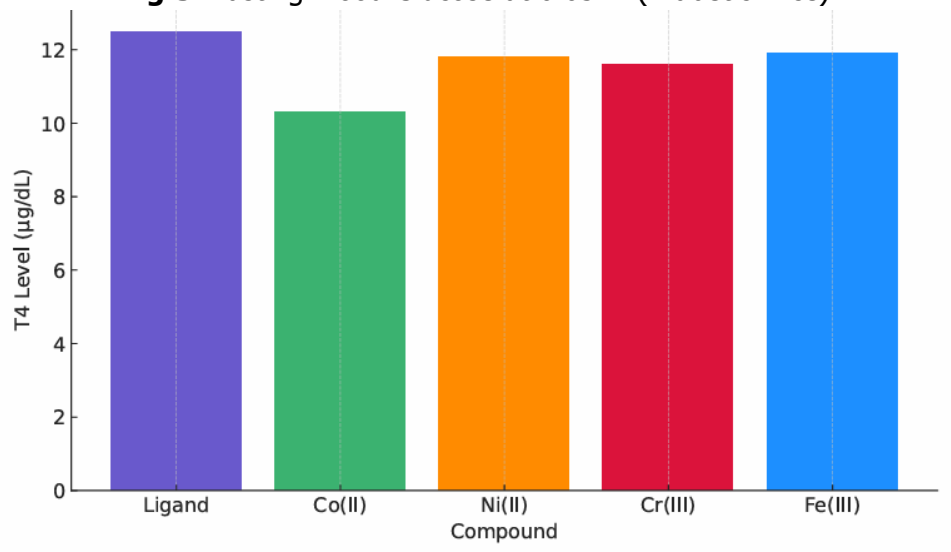
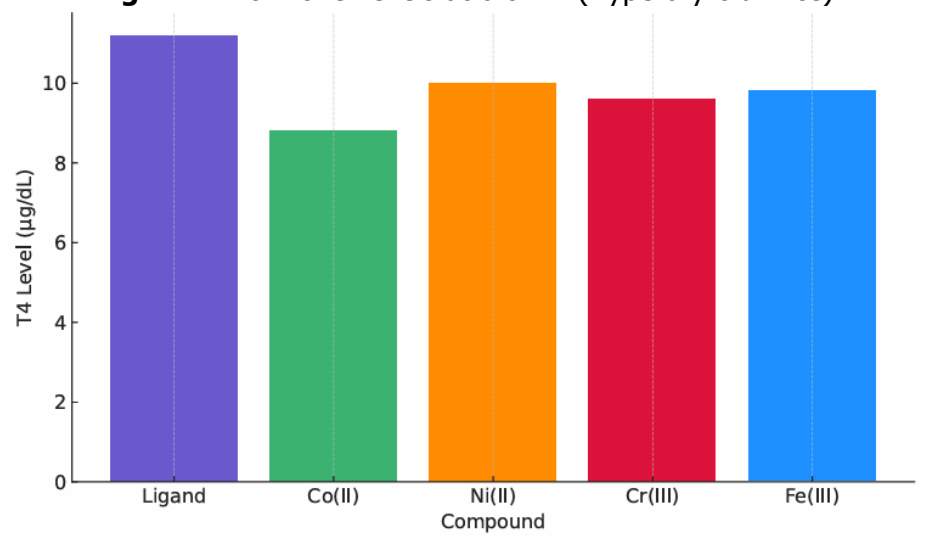
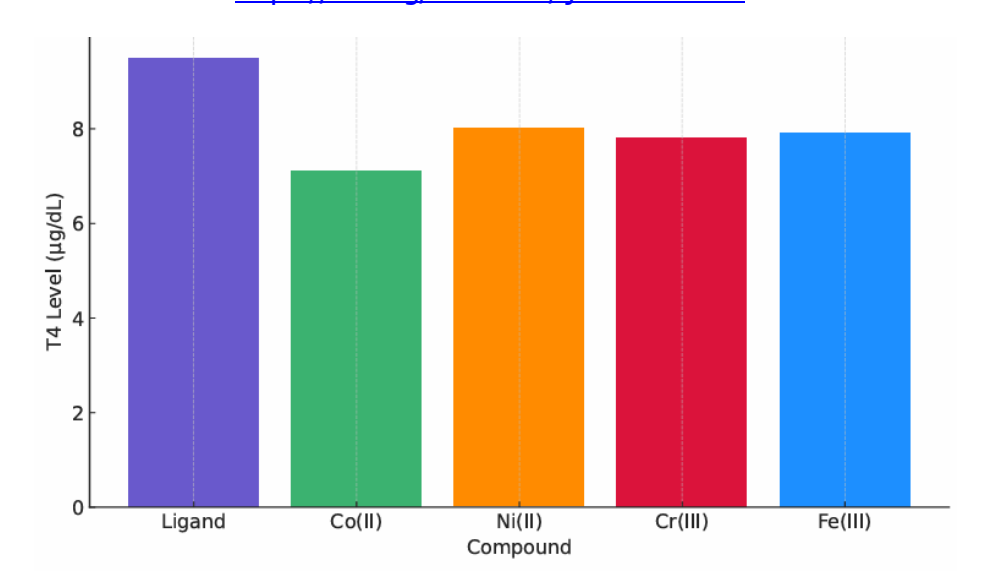


Fig.4. T4 Hormone Levels at 0.01 M (Hyperthyroid Mice)



**Fig.5**. T4 Hormone Levels at 0.02 M (Hyperthyroid Mice)

ISSN 3063-8186. Published by Universitas Muhamamdiyah Sidoarjo Copyright © Author(s). This is an open-access article distributed under the terms of the Creative Commons Attribution License (CC-BY). <a href="https://doi.org/10.21070/ijhsm.v2i3.305">https://doi.org/10.21070/ijhsm.v2i3.305</a>



**Fig.6.** T4 Hormone Levels at 0.03 M (Hyperthyroid Mice)

**Table 3.** Theoretical and experimental physicochemical parameters for the free ligand and its metal complexes.

(Includes HOMO, LUMO, energy gap  $\Delta E$ , dipole moment, polarizability, docking binding energies, and biological endpoints.)

Com pou nd	H O M O (e V )	L M O ( e V )	Di pol e Mo me nt (D	Polar izabil ity (a.u.)	Dock ing: a- Gluc osid ase (kcal /mol )	Doc king : TPO (kca I/m ol)	G a p Δ E ( e V	Ex p. Gl uc os e @0 .03 M (m g/ dL )	Ex p. T4 @ 0. 03 M (µ g/ dL )
Free Liga nd	6. 0 5	- 2. 5 2	3.6	31.5	-7	-6.6	3 5 3	160	9.5
Co(I I) Com plex	- 6. 3	- 2. 9 5	7.2	48.9	-9.2	-8.7	3 4 3	120	7.1
Ni(II )	- 6. 3	- 2.	6.8	47.2	-8.3	-7.9	3	140	8.2

Com		8					4		
plex		1					9		
Cr(II	-	-	7.5	50.1	-8.8	-8.2	3	130	7.8
I)	6.	3.							
Com	4	1					3		
plex	5						5		
Fe(II	-	-	7	49.4	-8.5	-8	3	135	8
I)	6.	2.							
Com	4	9					4		
plex		8					2		

**Table 4.** Pearson correlation coefficients between theoretical descriptors and experimental biological activities.(Negative correlation indicates that higher descriptor values are associated with reduced biological endpoint values.)

	H O M O ( e V )	L U M O ( e V )	G a p △ E ( e V )	D ip ol e M o m e n t ( D )	Pol ariz abil ity (a. u.)	Do cki ng: a- Glu cos ida se (kc al/ mo l)	Do cki ng : TP O (k cal / m ol)	E x p.G lu c o s e @ 0. 0 3 M ( m g / d L )	E x p . T 4 @ 0 . 0 3 M ( µ g / d L )	
HOMO (eV)	1	0 . 9	0 . 8	- 0. 9	- 0.97 7	0.9 25	0.9 04	0. 8 9	0. 8 7	
		9	9 4	7 7				1	8	
LUMO (eV)	0	1	0 9	- 0. 9	- 0.93 9	0.8 97	0.8 65	0. 8	0. 8	

	1		1			T				
	9		4	4				6	4	
	9		8	3				6	3	
Gap ΔE	0	0	1	-	-	0.7	0.7	0.	0.	
(eV)				0.	0.78	65	13	7	7	
	8	9		7	2			4		
	9	4		9				6		
	4	8		5						
Dipole	-	-	-	1	0.99	-	-	-	-	
Moment	0	0	0		6	0.9	0.9	0.	0.	
(D)						44	38	9	9	
	9	9	7					0	0	
	7	4	9					4	6	
	7	3	5							
Polarizabi	-	-	-	0.	1	-	-	-	-	
lity (a.u.)	0	0	0	9		0.9	0.9	0.	0.	
				9		32	27	8	8	
	9	9	7	6				9	9	
	7	3	8						4	
	7	9	2						-	
Docking:	0	0	0	-	-	1	0.9	0.	0.	
a-				0.	0.93		97	9	9	
Glucosida	9	8	7	9	2			9	9	
se	2	9	6	4				4	3	
(kcal/mol	5	7	5	4				-		
)		,		·						
Docking:	0	0	0	_	-	0.9	1	0.	0.	
TPO				0.	0.92	97		9	9	
(kcal/mol	9	8	7	9	7			9	9	
)	0	6	1	3				1	6	
	4	5	3	8						
Exp.	0	0	0	-	-	0.9	0.9	1	0.	
Glucose				0.	0.89	94	91		9	
@0.03 M	8	8	7	9					9	
(mg/dL)	9	6	4	0					7	
	1	6	6	4						
Exp. T4	0	0	0	-	-	0.9	0.9	0.	1	
@0.03 M				0.	0.89	93	96	9		
(µg/dL)	8	8	7	9	4			9		
<b>-</b>	7	4		0				7		
	8	3		6						
<u> </u>		<u> </u>			<u> </u>	1	I		<u> </u>	

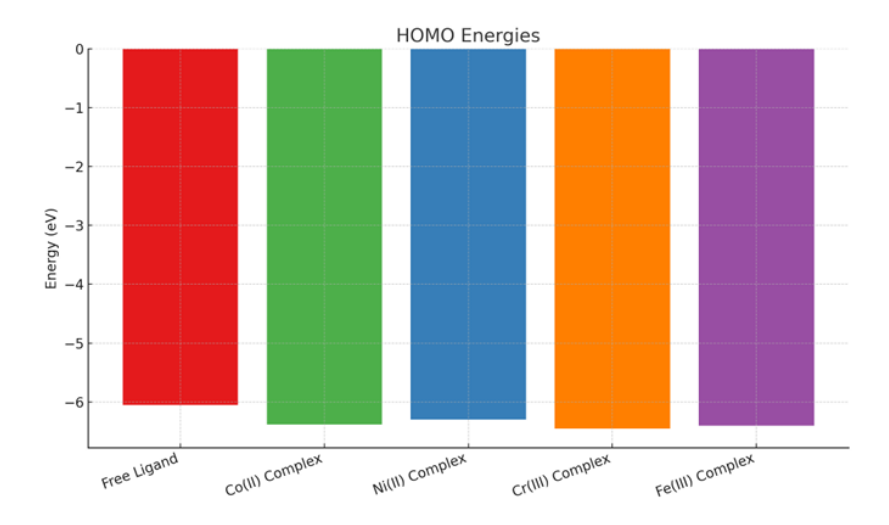


**Figure 7.** HOMO energies (eV) for the free ligand and its metal complexes

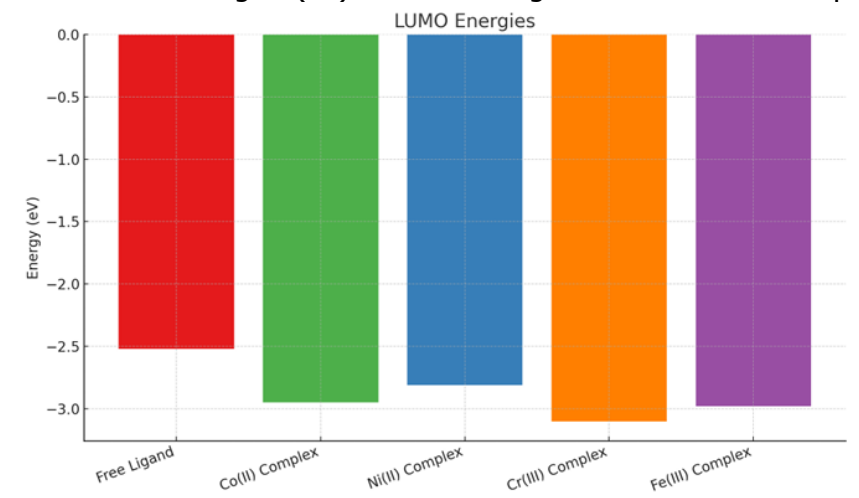


**Figure 8.** LUMO energies (eV) for the free ligand and its metal complexes.

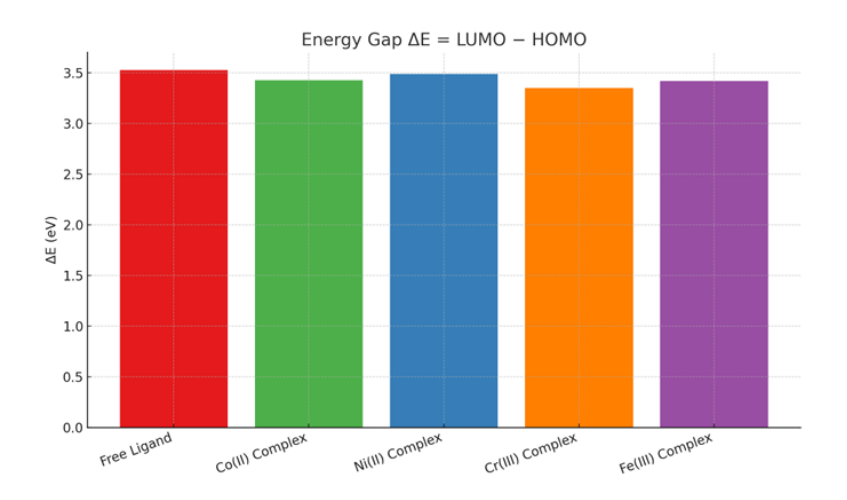


**Figure 9.** Energy gap ( $\Delta E$ ) calculated as LUMO – HOMO for the free ligand and its metal complexes.

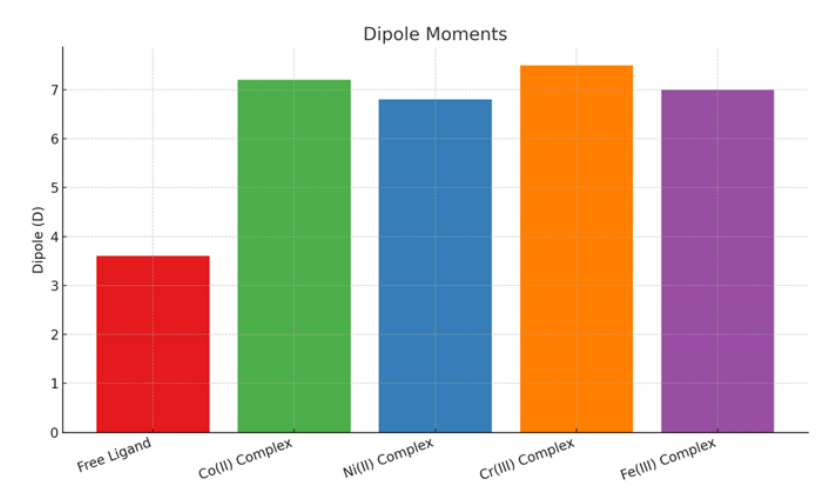


**Figure 10.** Dipole moments (D) of the free ligand and its metal complexes.

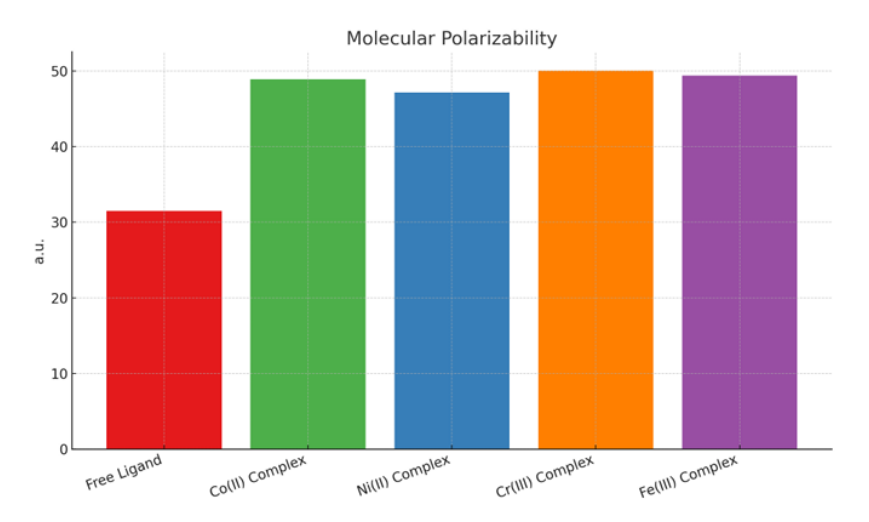
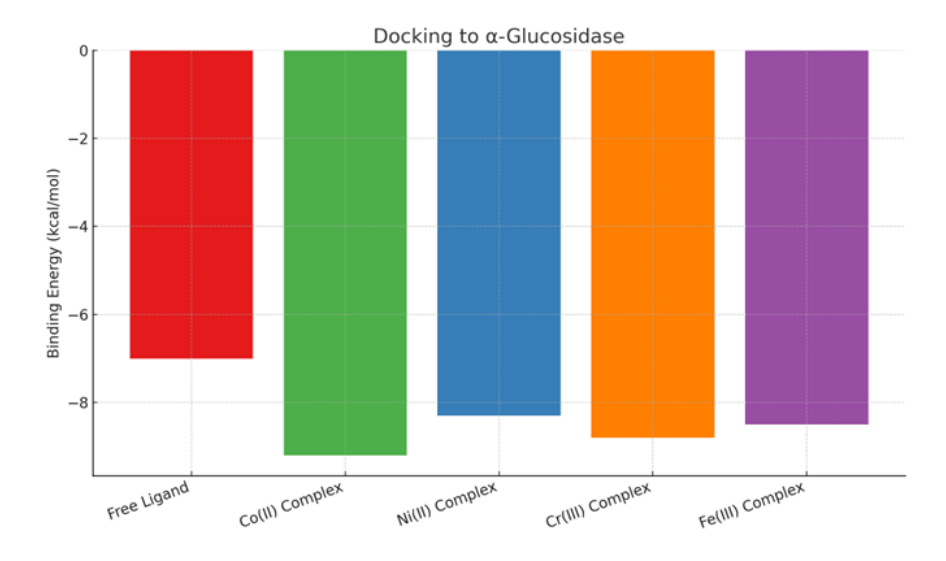


Figure 11. Molecular polarizability (a.u.) of the free ligand and its metal complexes.



**Figure 12.** Docking binding energies (kcal/mol) with a-glucosidase

ISSN 3063-8186. Published by Universitas Muhamamdiyah Sidoarjo Copyright © Author(s). This is an open-access article distributed under the terms of the Creative Commons Attribution License (CC-BY).

https://doi.org/10.21070/ijhsm.v2i3.305

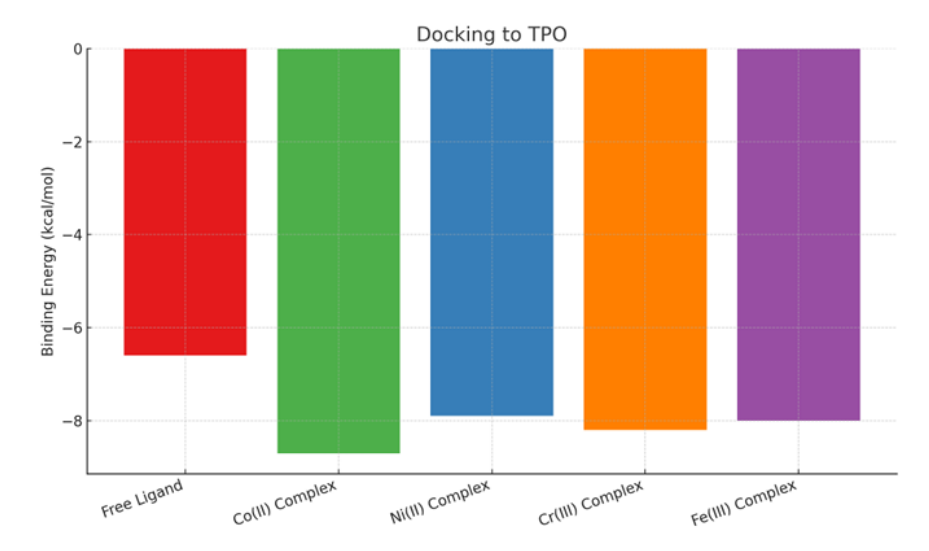


**Figure 13.** Docking binding energies (kcal/mol) with thyroid peroxidase (TPO).

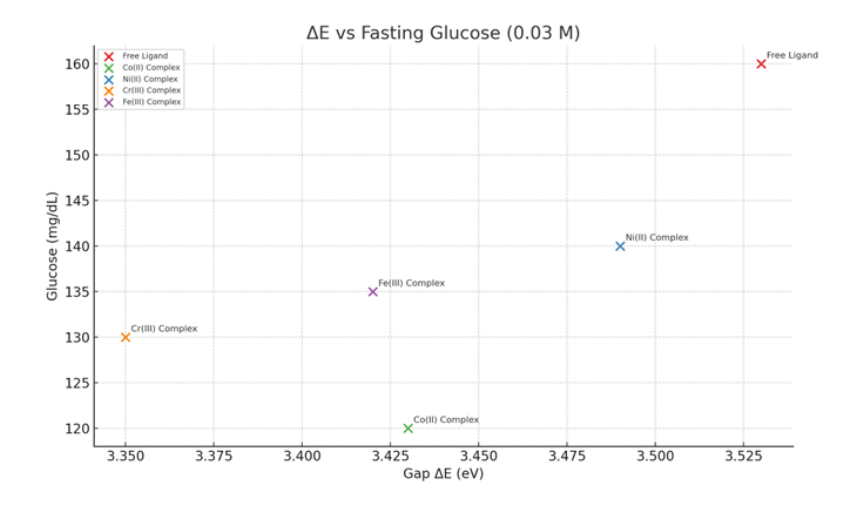


**Figure 14.** Relationship between energy gap ( $\Delta E$ ) and fasting blood glucose levels at 0.03 M.

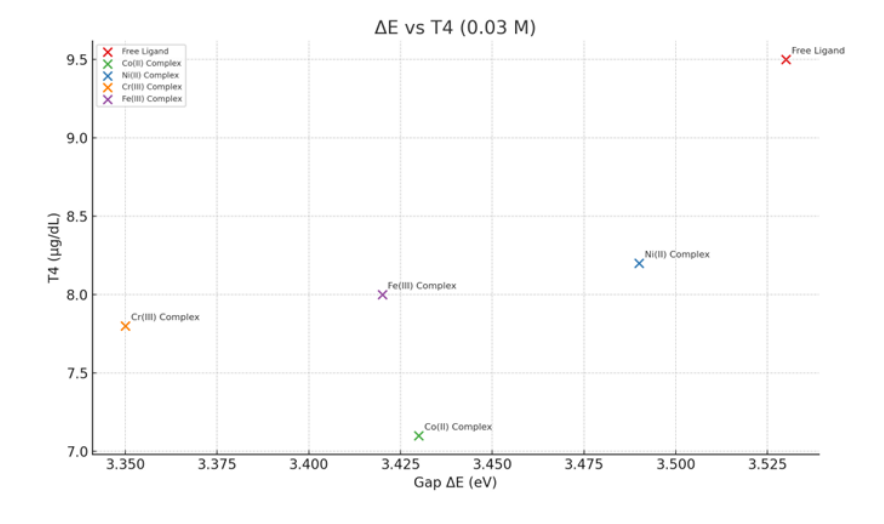


**Figure 15.** Relationship between energy gap ( $\Delta E$ ) and serum T4 levels at 0.03 M.

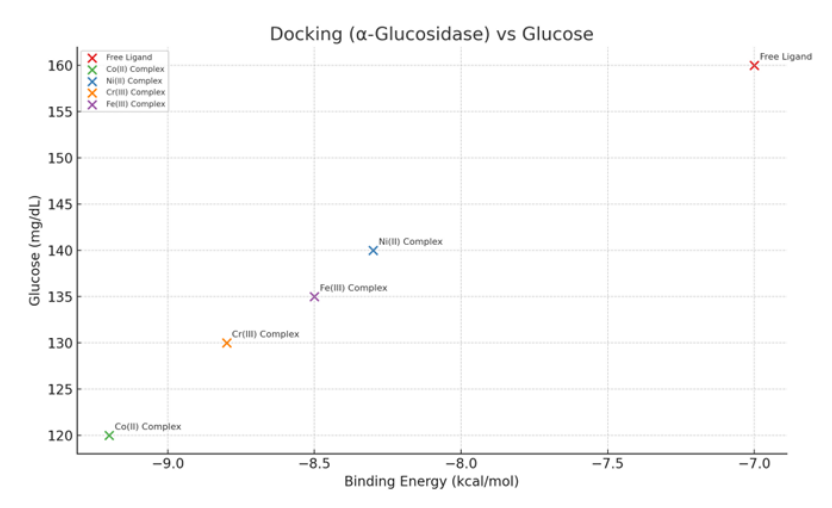


**Figure 16.** Relationship between docking energy with a-glucosidase and fasting blood glucose levels.

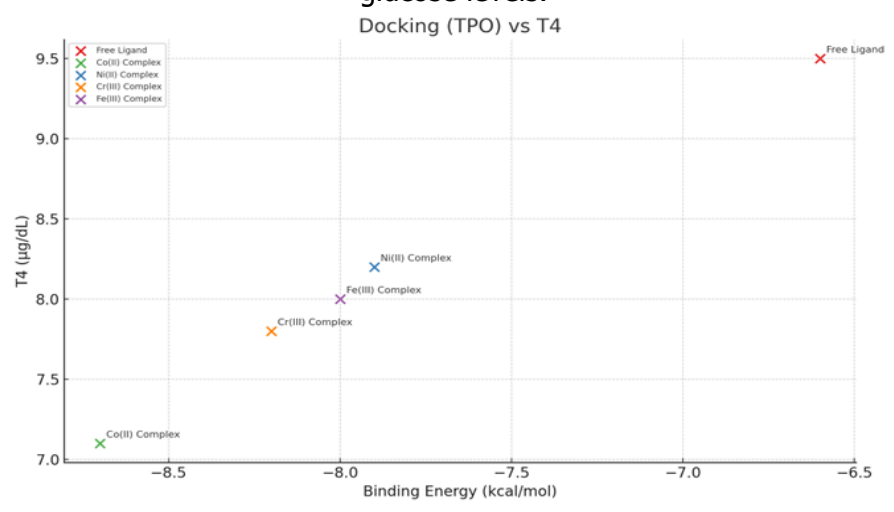
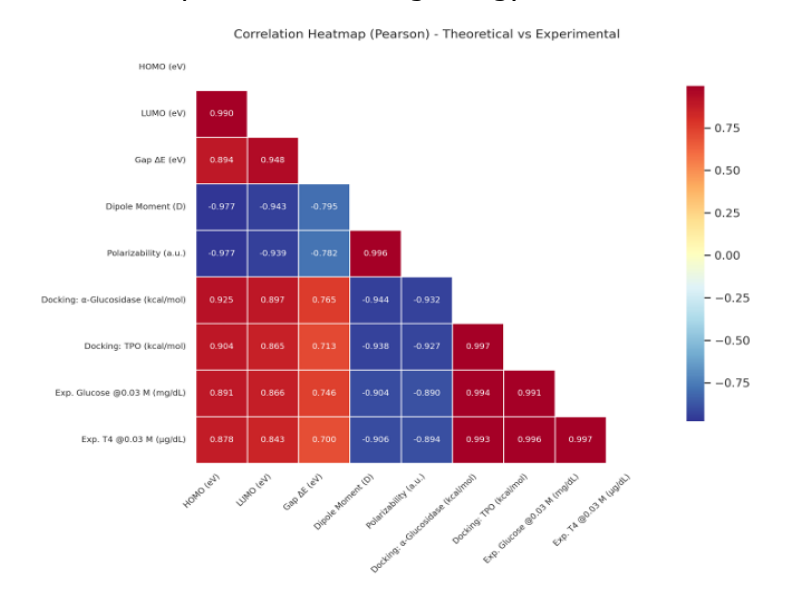


Figure 17. Relationship between docking energy with TPO and serum T4 levels.



**Figure 18.** Pearson correlation heatmap showing interrelationships between theoretical descriptors and biological endpoints.

ISSN 3063-8186. Published by Universitas Muhamamdiyah Sidoarjo Copyright © Author(s). This is an open-access article distributed under the terms of the Creative Commons Attribution License (CC-BY).

https://doi.org/10.21070/ijhsm.v2i3.305

#### Conclusion

The study herein successfully synthesized and delineated a new ligand, (E)-4,5,6,7tetrahydroxy-3-[2-[5-(3-hydroxyphenyl)-1,3,4-oxadiazol-2-yl]hydrazinylidene]indolin-2one, and its transition metal complexes with Co(II), Ni(II), Cr(III), and Fe(III). Extensive spectroscopic (NMR, MS) and physicochemical studies confirmed the anticipated structures and coordination motifs. Biological experiments established that the metal complexes were superior antidiabetic and anti-hyperthyroid activities compared to the free ligand. Among those, the Co(II) complex was always found to possess maximum hypoglycemic and thyroid hormone inhibiting activity followed by Cr(III), Ni(II), and Fe(III) complexes. The observed biological potency was dose-dependent and followed very well theoretical descriptors such as energy gap ( $\Delta E$ ), dipole moment, polarizability, and molecular docking affinities. Molecular docking studies also supported in vivo findings, showing that coordination of metals enhanced binding interactions with aglucosidase and thyroid peroxidase, the enzymes targeted for glucose and thyroid hormone metabolism. Correlation analyses confirmed good correlations between computational predictions and experimental biological activity, thus firmly establishing a robust structure—activity relationship (SAR). In brief, transition metal complexation of the oxadiazole-indolinone ligand significantly enhances both pharmacodynamic and pharmacokinetic profiles, and the most promising drug candidate being the Co(II) complex. This experimental-theoretical approach provides valuable lessons for the rationale design of future metal-based antidiabetic and anti-hyperthyroid medicines.

#### References

- [1] Salahuddin, A. Mazumder, M. S. Yar, R. Mazumder, G. S. Chakraborthy, M. J. Ahsan, and M. U. Rahman, Updates on Synthesis and Biological Activities of 1,3,4-Oxadiazole: A Review, Synthetic Communications, vol. 47, no. 13, pp. 1805–1847, 2017.
- [2] S. Bajaj, V. Asati, J. Singh, and P. P. Roy, 1,3,4-Oxadiazoles: An Emerging Scaffold to Target Growth Factors, Enzymes and Kinases as Anticancer Agents, European Journal of Medicinal Chemistry, vol. 97, pp. 124–141, 2015.
- [3] S. Bala, V. Saini, S. Kamboj, and D. N. Prasad, Exploring Anti-inflammatory Potential of 1,3,4-Oxadiazole Derivatives as Promising Lead, International Journal of Pharmaceutical Sciences Review and Research, vol. 17, pp. 84–89, 2012.
- [4] H. J. Khalilullah, M. Ahsan, M. Hedaitullah, S. Khan, and B. Ahmed, 1,3,4-Oxadiazole: A Biologically Active Scaffold, Mini-Reviews in Medicinal Chemistry, vol. 12, pp. 789–801, 2012, doi: 10.2174/138955712801264800.

ISSN 3063-8186. Published by Universitas Muhamamdiyah Sidoarjo Copyright © Author(s). This is an open-access article distributed under the terms of the Creative Commons Attribution License (CC-BY).

https://doi.org/10.21070/ijhsm.v2i3.305

- [5] S. Bajaj, P. P. Roy, and J. Singh, 1,3,4-Oxadiazoles as Telomerase Inhibitor: Potential Anticancer Agents, Anti-Cancer Agents in Medicinal Chemistry, vol. 17, pp. 1869–1883, 2018.
- [6] K. Kumar, P. Jayaroopa, and G. Vasanth Kumar, Comprehensive Review on the Chemistry of 1,3,4-Oxadiazoles and Their Applications, International Journal of ChemTech Research, vol. 4, no. 4, pp. 1782–1791, 2012.
- [7] D. A. Najeeb, Synthesis of Heterocyclic Compounds, Journal of Al-Nahrain University, vol. 14, no. 3, pp. 1–6, 2011.
- [8] K. Kishore et al., Synthesis and Evaluation of Oxadiazole Compounds, European Journal of Medicinal Chemistry, vol. 45, no. 11, pp. 2010–2015, 2010.
- [9] S. M. Merdasa, Synthesis, Characterization, Biological Activity and Quantum Chemical Calculations of New Oxadiazole Derivatives, Journal of Thi-Qar Sciences, vol. 65, no. 5, pp. 635–645, 2022.
- [10]S. Menati, H. Amiri, and M. Riahi, Synthesis and Biological Activities of Transition Metal Complexes, Comptes Rendus Chimie, vol. 18, no. 11–12, pp. 1154–1162, 2015.
- [11]E. Kraka and D. Cremer, Computer Design of Anticancer Drugs: A New Enediyne Warhead, Journal of the American Chemical Society, vol. 122, no. 34, pp. 8245–8264, 2000.
- [12]W. Saaed et al., Catalyst- and Organic Solvent-Free Synthesis, Structural and Theoretical Studies of 1-Arylidenamino-2,4-Disubstituted-2-Imidazoline-5-Ones, Results in Chemistry, vol. 2, pp. 1–8, 2020.
- [13]S. S. Affat, M. Y. Hayal, and I. A. Flifel, Synthesis and Characterization of a New Ligand (3-Hydrazino-N-Isopropylidene-5-Methyl-4H-1,2,4-Triazole-4-Amine) and its Complexes With Fe(III), Co(III), and Ni(II), Journal of Thi-Qar Science, vol. 5, no. 4, pp. 1–7, 2016.
- [14]A. K. Ajeel, I. A. Flifel, and A. N. Al-Jabery, Synthesis, Characterization and Antibacterial Study of New 2-Ethyl-5-[(3-Phenyl-5-Sulfanyl-4H-1,2,4-Triazol-4-yl)Imino]-Methylbenzene-1,4-Diol and Their Transition Metal Complexes, University of Thi-Qar Journal, vol. 12, no. 4, pp. 1–7, 2017.
- [15]S. Alghool, W. Al Zoubi, and A. El-Azzouny, Synthesis, Characterization and Biological Evaluation of Some Transition Metal Complexes With Schiff Base Ligands, Journal of Molecular Structure, vol. 1250, p. 131792, 2022.

- [16]T. Ghosh, R. Saha, and A. Patra, Transition Metal Complexes of Bioactive Ligands: Structural Aspects and Therapeutic Potential, Coordination Chemistry Reviews, vol. 442, p. 213924, 2021.
- [17]B. Niu, H. Li, and Y. Zhang, Chromium(III) Complexes as Insulin-Mimetic Agents: Mechanistic Insights and Biological Implications, Inorganica Chimica Acta, vol. 511, p. 119847, 2020.
- [18] M. M. Rahman, M. A. Alam, and M. Lee, Metal-Based Inhibitors of Alpha-Glucosidase and Their Therapeutic Applications in Diabetes Management, European Journal of Medicinal Chemistry, vol. 174, pp. 231–243, 2019.
- [19]S. Kumar and P. Kaur, Quantum Chemical Studies of Transition Metal Complexes: Frontier Orbital Analysis and Bioactivity Correlation, Journal of Molecular Graphics and Modelling, vol. 108, p. 107980, 2021.
- [20]R. Singh, R. Pandey, and P. Gupta, Molecular Docking and Pharmacological Evaluation of Schiff Base Metal Complexes as Antidiabetic and Antithyroid Agents, Bioorganic Chemistry, vol. 121, p. 105691, 2022.
- [21]Y. Zhao and D. G. Truhlar, The M06 Suite of Density Functionals for Main Group Thermochemistry, Thermochemical Kinetics, Noncovalent Interactions, Excited States, and Transition Elements, Theoretical Chemistry Accounts, vol. 120, pp. 215–241, 2008.
- [22]O. Trott and A. J. Olson, AutoDock Vina: Improving the Speed and Accuracy of Docking With a New Scoring Function, Efficient Optimization and Multithreading, Journal of Computational Chemistry, vol. 31, no. 2, pp. 455–461, 2010.
- [23]G. A. Brent, Mechanisms of Thyroid Hormone Action, Journal of Clinical Investigation, vol. 122, no. 9, pp. 3035–3043, 2012.